



OPEN ACCESS

EDITED BY

Jung Ho Kim,
University of Wollongong, Australia

REVIEWED BY

Jongsoo Kim,
Sungkyunkwan University Suwon, Republic of
Korea
Ruhong Li,
Zhejiang University, China

*CORRESPONDENCE

Janghyuk Moon,
✉ jhmoon84@cau.ac.kr

RECEIVED 12 October 2025

REVISED 04 November 2025

ACCEPTED 24 November 2025

PUBLISHED 19 December 2025

CITATION

Tham BT, Park S, Chang H, Moon T and Moon J
(2025) Innovative approaches in cathode
material selection: high-throughput
computational screening for anode-free zinc
battery and beyond.
Front. Batter. Electrochem. 4:1723256.
doi: 10.3389/fbael.2025.1723256

COPYRIGHT

© 2025 Tham, Park, Chang, Moon and Moon.
This is an open-access article distributed under
the terms of the [Creative Commons Attribution
License \(CC BY\)](#). The use, distribution or
reproduction in other forums is permitted,
provided the original author(s) and the
copyright owner(s) are credited and that the
original publication in this journal is cited, in
accordance with accepted academic practice.
No use, distribution or reproduction is
permitted which does not comply with these
terms.

Innovative approaches in cathode material selection: high-throughput computational screening for anode-free zinc battery and beyond

Bui Thi Tham, Seongsoo Park, Hongjun Chang, Taejoon Moon and Janghyuk Moon*

Department of Energy Systems Engineering, Chung-Ang University, Seoul, Republic of Korea

Aqueous zinc-based batteries (AZBs) stand at the forefront of aqueous energy storage technologies, boasting high degree of energy density and economics. Although the advantages of Zinc electrochemical potential and theoretical capacity, challenges such as dendrite growth and cycling inefficiencies persist because of the use of excess zinc in thick metal anodes. An emerging solution lies in anode-free zinc batteries (AFZB), which leverage Zn-rich cathode materials, eliminating the need for a zinc metal anode. This approach optimizes weight reduction to elevate performance and achieve superior energy density. However, it mandates a cathode equipped with a substantial Zinc ratio, robust structure, and favorable diffusion kinetics. Employing a high-throughput computational screening technique tailored for zinc-rich cathodes within the $Zn_{TM_x}A_y$ domain, we have pinpointed six highly promising compounds from an initial pool of 1,005 structures. This breakthrough signifies substantial progress in the next-generation energy storage systems, particularly within the domain of anode-free zinc batteries, poised to catalyze a profound paradigm shift in battery technology.

KEYWORDS

anode-free zinc battery, zinc-rich cathode materials, high-throughput computational screening, thermo-electrochemical stability, aqueous stability, zn-ion diffusion kinetics

1 Introduction

The field of energy storage through battery systems is experiencing robust development driven by real-world demands in current and future applications. Research and development efforts in lithium-ion batteries highlight unfortunate limitations, primarily due to the scarcity of lithium metal, along with safety issues that organic electrolytes in Li-ion systems can undergo thermal runaway under abuse conditions, posing safety concerns, impeding their commercialization potential (Fang et al., 2018). Recently, researchers have shifted their focus towards exploring alternative battery systems that meet the requirements of energy storage, safety, and reduced production costs. Within the emerging technologies, aqueous zinc batteries (AZBs) have garnered consideration for zinc is abundant, inexpensive, and environmentally friendly, contributing to lower production costs compared to lithium-ion batteries. Additionally, aqueous electrolytes are inherently safer than the organic electrolytes utilized in a good deal of battery types with lithium ion, lowering the possibility of thermal overheating and fire hazards (Song et al., 2018). Typically, AZBs are designed with zinc metal serving as the anode, a crucial component that

significantly determines the battery performance. Zinc exhibits an attractive electrochemical potential that ranges around -0.76 V (vs. SHE), indicating its ability to efficiently undergo oxidation-reduction reactions during battery operation. Moreover, zinc boasts a substantial theoretical capacity of around 840 mA-hours per gram (mAh g^{-1}), which denotes total amount of charge that can be held for each mass of zinc. This high theoretical capacity implies that zinc has the potential to store a significant amount of energy within the battery system (Blanc et al., 2020; Li et al., 2020; Jia et al., 2020; Cao et al., 2022). Despite advancements in performance, the widespread use of thick zinc foils exacerbates the challenge of the instability in zinc anode, which remains a significant obstacle in the commercialization of AZBs (Blanc et al., 2020; Li et al., 2022). One issue stemming from the use of thick zinc foils is the accumulation of excessive zinc surplus in the anode (Du et al., 2022). These surplus limits the real energy density of the battery technology. Additionally, controlling the Zn^{2+} ion plating/stripping process poses challenges. When zinc ions plate onto and strip from the anode during charge and discharge cycles, irregularities can occur. These irregularities can lead to reduced cycle efficiency and rapid dendrite growth across the entire battery system (Zhang et al., 2021; Ming et al., 2022). Dendrite growth is the creation of branch-like structures on the surface of a zinc anode. These dendrites can penetrate the separator among the anode side and the cathode resulting in shorts in the circuit and potentially causing safety hazards such as thermal runaway or even fire (Kundu et al., 2016). Addressing these challenges is crucial for the successful commercialization of AZBs. Researchers are exploring various strategies to mitigate the instability of the zinc anode, including optimizing electrode design, developing new electrolytes, and employing protective coatings on the zinc surface. However, these strategies face challenges related to cost and the ability to scale up production (Zheng et al., 2019; Wang et al., 2018; Zhao et al., 2019). Recently, there has been interest in a new approach known as Anode-Free Zinc Batteries (AFZB) (An et al., 2021). Unlike traditional batteries that utilize a zinc metal anode, AFZB utilize zinc-rich cathode materials to supply Zn^{2+} ions during operation. This eliminates the necessity for a zinc metal anode altogether (Lin et al., 2022; Qian et al., 2016; Zhu et al., 2021). Researchers have been enhancing the performance of AFZB by applying a nano-carbon layer onto the copper foil (current collector), to ensure that the zinc layer is distributed evenly. This even distribution helps to optimize the performance of battery, resulting in an efficiency of 99.6% in Coulombic processes (Xie et al., 2020; Gong et al., 2014). A high CE indicates that a large percentage of the charge put into the battery during charging is effectively stored and retrieved during discharge, reflecting the efficiency of the battery in retaining a charge. Another approach involves utilizing copper foil with a thin coating of silver on top as an anode substrate. This technique was found to efficiently prevent the production of dendrites, which are unwanted growths that can develop on the electrode surfaces (Wang et al., 2022). The elimination of the zinc metal anode helps reduce weight and volume, thus increasing energy density. Additionally, it prevents passive electrode reactions and hydrogen formation, improving the cycling efficiency of AFZB (Zhang et al., 2022). The crucial role of the cathode material in AFZB, influencing overall power, cycle stability, and rate performance, requires the development of zinc-rich negative electrodes with a reliable source of Zn^{2+} ions and simple

processes. These electrodes should exhibit superior electrochemical properties such as high energy density, robust structure, and efficient diffusion kinetics to fully unleash the potential of AFZB (Zhao et al., 2020; Liu and Wu, 2022; Yang et al., 2022; Guo et al., 2021).

In recent studies, various zinc-rich cathode materials have been investigated. Leveraging the understanding gained from LiMn_2O_4 , researchers initially expected that ZnMn_2O_4 could serve as a promising source of zinc for battery applications. However, the intact spinel structure of ZnMn_2O_4 , characterized by tightly bound zinc and manganese ions within the crystal lattice, creates obstacles to the movement of zinc ions. Consequently, the removal of Zn^{2+} ions from cathode materials proceeds at a slower pace, resulting in sluggish kinetics. Furthermore, the reversible process of extracting and reinserting zinc ions into the cathode material is constrained, impeding the ability to maintain battery performance over repeated charge-discharge cycles (Knight et al., 2015). In a notable advancement, researchers developed a cation-deficient $\text{ZnMn}_2\text{O}_4/\text{C}$ cathode specifically tailored for AZBs. This modified cathode outperforms the pristine version due to the abundance of Mn vacancies inside its structure. These vacancies give extra places for zinc ions to intercalate, improving the total capacity and efficiency in the battery (Zhang et al., 2016; Zhang et al., 2019). Similarly, zinc cobalt dioxide (ZnCo_2O_4) has gained interest as a cathode component for “rocking-chair” Zn-ion battery. However, the direct use of pure ZnCo_2O_4 as a cathode material faces challenges due to its instability in aqueous electrolytes commonly used in Zn-ion batteries. To address this issue, researchers have explored the strategy of substituting metal ions within the ZnCo_2O_4 structure to enhance its compatibility with electrolytes. In a study conducted in 2017, researchers reported the synthesis of aluminum-doped ZnCo_2O_4 ($\text{ZnAl}_x\text{Co}_{2-x}\text{O}_4$), where aluminum (Al) ions were incorporated into the ZnCo_2O_4 lattice. Specifically, they investigated the composition $\text{ZnAl}_{0.67}\text{Co}_{1.33}\text{O}_4$, which demonstrated promising electrochemical performance. This material has a high working voltage and excellent stability during cycling, with a specific capacity of 114 mAh/g after 100 cycles (Pan et al., 2017). Furthermore, another approach to enhancing the performance of ZnCo_2O_4 involves co-doping with manganese (Mn) and nickel (Ni) ions. By introducing Mn and Ni into the ZnCo_2O_4 structure, creating the $\text{ZnNi}_x\text{Mn}_x\text{Co}_{2-2x}\text{O}_4$ cathode material, showed the capacity to sustain cycle performance and reached a high voltage of 2.05 V in the open circuit after 200 cycles (Chen et al., 2020). Furthermore, because of its high working voltage (2.0 V) and three-dimensional open-framework structure, zinc hexacyanoferrate has attracted a lot of interest (Chen et al., 2020; Zhang et al., et al., 2019; Kasiri et al., 2019). Recently, a spinel $\text{Zn}_3\text{V}_3\text{O}_8$ was identified as the first vanadium-based material for a unique Zn-metal-free AZB, with a discharge capacity of 127 mAh/g (Wu et al., 2021). Notwithstanding these advances, the majority of progress toward Zn-based cathodes in batteries is based on conventional experimental approaches. This approach unavoidably extends the time and cost required for the development of new electrodes, ultimately resulting in insufficient efficiency (Cai et al., 2022; Wang et al., 2021; Wang et al., 2015).

In recent years, advancements in computer techniques and theoretical models have efficiently facilitated the exploration of energy storage mechanisms in new electrode materials.

Extensively documented high-throughput screening techniques for materials have the potential to drastically cut down on the time and expense required to produce innovative materials (Curtarolo et al., 2013; Curtarolo et al., 2012; Kahle et al., 2020; Ricci et al., 2020). The combined screening processes with DFT calculations were used to investigate cathode materials for Li-O₂ batteries, considering stability, band gap, surface energy, and oxygen adsorption ability. Out of the 2,800 structures examined, 33 interesting compounds with low surface energy were discovered (Boev et al., 2021). A high-throughput technique, along with machine learning, was employed to screen cathode materials with Mg/Zn components for application in organic batteries. This strategy led to the discovery of six novel spinel materials distinguished by strong conductivity, rapid ion diffusion, and low-volume increase rates (Cai et al., 2021). Similarly, high-throughput screening of spinel cathode materials for AZBs revealed 14 candidates from 12,047 Mn/Zn-O-based materials based on structural assessment and critical electrode characteristics. Subsequent evaluations through first-principles calculations resulted in the identification of five potential candidates (Luo et al., 2023). In this study, design rules for a high-throughput computational screening process have been developed to identify zinc-based cathode materials for AFZB from the Materials Project database. The methodology involves a four-stage screening procedure, sequentially selecting the most promising candidates based on their thermodynamic stability, electrical conductivity, voltage with capacity, and aqueous stability. The screening process specifically targets zinc-rich cathodes within the Zn-TM_xA_y category, where TM comprises (post-)transition metals like Co, Ni, Cu, Y, Zr, Nb, Sc, Ti, V, Mn, Mg, Fe, Mo, Tc, Ru, Ag, and A represents anions like O, S, N, Se, Te, F, B, C, Si, P, As, Ge. This exhaustive screening found six candidate compounds from an original pool of 1,005 structures. This substantial innovation represents a critical step forward in advancing the creation of zinc-rich cathodes for large-scale energy storage systems, particularly for battery applications that do not require zinc anodes.

2 Materials and methods

2.1 Thermodynamic stability

The stability of zinc-rich cathode materials is vital across diverse applications, with assessment revolving around their resilience to energy fluctuations during atomic rearrangements. One common phenomenon affecting stability is phase separation, where a material can form competing stable materials or undergo a phase transition while maintaining its composition (Bartel, 2022). To investigate the stability of zinc-rich cathodes undergoing phase separation, researchers use methods like the convex hull geometric method. The above-hull energy (ΔE_{hull}) serves as a characteristic quantity for dynamic thermodynamic stability, indicating a propensity for separation or phase transition of compounds (Wang et al., 2021). Thermodynamically stable materials have ΔE_{hull} equal 0, and their decomposition energy with negative value indicates the degree of stability. According to statistical data from most computational studies, solid phases are potentially synthesizable when their ΔE_{hull} is less than 25 meV/atom (Young et al., 2023; Sun et al.,

2016; Cerqueira et al., 2015; Aykol et al., 2018; Hautier et al., 2012). Therefore, zinc-rich cathode materials with ΔE_{hull} values less than 25 meV/atom are selected as materials for AFZB. For chemical systems with multiple components, thermodynamic phase equilibria are depicted through points on a phase diagram with specific energy values. To efficiently construct a phase diagram for compounds, computational methods, particularly density functional theory (DFT), are widely utilized, as demonstrated comprehensively in the database of Materials Project. The development of a phase diagram for a chemical system (e.g., a system composed of elements Zn-TM-A) involves calculating the ground-state energy for all relevant compounds under fixed conditions of $T = 0\text{K}$ and $P = 0\text{ atm}$ (Ong et al., 2008). This computational approach has been integrated into Python algorithms through the Pymatgen package to compute dynamic stability, formation energy, and energy on the convex hull for each material based on its phase diagram (Bartel, 2022).

2.2 Electrical conductivity

The band theory stands as a pivotal framework in comprehending the electronic structure of materials and their electrical characteristics. The capacity of electrons to traverse these energy bands, or the absence thereof, determines whether a material functions as an insulator, semiconductor, or conductor. Band gap indicates the energy needed for an electron to go from the band called valence into the band of conduction in terms of electrical conductivity (Park et al., 2021). In materials with large band gaps (greater than 2 eV), the substance tend to act as an insulator. Materials with small band gaps are semiconductors, whereas conductors have band gaps close to 0 eV (Xie et al., 2017). In semiconductors, some electrons can get sufficient thermal energy at room temperature to transition between energy bands, generating electric charge carriers. Therefore, our screening process relies on materials with energy band gaps less than or equal to 2 eV, suitable for applications involving a zinc-rich cathode in AFZB (Shen et al., 2025; kabiraj et al., 2022).

2.3 Electrochemical stability within H₂ and O₂ evolution

In zinc-rich cathode materials, lattice anions do not actively participate in the redox (reduction-oxidation) processes that take place during electrochemical reactions. Despite their presence in the crystal lattice, these anions typically remain relatively inert in terms of electron transfer (Xie et al., 2017). The procedure of determining the average potential of zinc (Zn) intercalation into a cation TM material, concerning Zn/Zn²⁺, follows a similar Equation 1,

$$V = -\frac{E_{\text{DFT}}(\text{Zn}_m\text{M}) - E_{\text{DFT}}(\text{Zn}_{m-x}\text{M}) - xE_{\text{DFT}}(\text{Zn})}{xF} \quad (1)$$

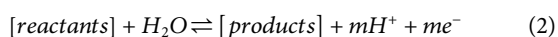
This equation involves parameters such as the total energy obtained through density functional theory (DFT), denoted as E_{DFT} , and m represents the electron charge (Aydinol et al., 1997). The average intercalation potential is crucial for understanding and optimizing the performance of zinc-rich cathode materials in

electrochemical systems. Voltage profiles are generated by utilizing stable phases identified from the phase diagram of a compound when Zn is intercalated and extracted (Bartel, 2022). This method assesses the thermodynamic stability of different compositions and aids in understanding the intercalation behavior of Zinc. The initial structures for Zn-intercalated phases are obtained either from the Materials Project (Jain et al., 2013). To identify partly extracted structures, all symmetrically different placings inside large super cells are enumerated. This process streamlined using the library adaptor as implemented in Pymatgen (Hart and Forcade, 2008; Ong et al., 2013). For each compound, a minimum of 20 combinations with the lowest electrostatic energy, as measured by the Ewald summation technique, are selected. These arrangements are then utilized in constructing the convex hull, providing insights into the thermodynamic stability and voltage characteristics during the Zinc intercalation process.

A suitable operational potential lies within the range of potentials for hydrogen (H₂) and oxygen (O₂) evolution, which typically spans between 0.347 and 1.576 V versus Zn/Zn²⁺ inside a neutral solution (Zanatta, 2019). Notably, when considering practical energy densities as reported in the literature, the average operational potential tends to be higher versus Zn/Zn²⁺ in a neutral electrolyte. This higher operational potential is crucial for achieving the desired energy density in practical applications (Aydinol et al., 1997).

2.4 Aqueous stability

Aqueous stability based on Pourbaix diagrams involves assessing the thermodynamic stability of materials in each chemical system, particularly electrochemical reactions occurring in aqueous environments. Pourbaix diagrams are used to represent the thermodynamic stability of various chemical species concerning pH and electrode potential. Pourbaix diagrams are created using the exacting process described by Persson et al., smoothly combine observed aqueous reference phase with ab initio-calculated stages of solids (Persson et al., 2012). Within the chemical complex denoted as Zn-TM-A, the identification of Pourbaix stable domains is an intricate process that involves exploring all potential equilibrium redox reactions within the expansive Zn-TM-A-O-H chemical space.



Equation 2 encapsulates a dynamic reaction unfolding in an aqueous medium at a specific pH, where reactants and H₂O collaborate to yield products, accompanied by the creation of mH⁺ ions and me⁻ electrons.

$$-nEF = \Delta G_r = \Delta G_r^0 - 2.303RT \, m \, \text{pH} + 2.303RT \log \frac{[\text{reactant}]}{[\text{product}]} \quad (3)$$

The Nernst Equation 3 explains the manner in which changes in external potential affect the thermodynamics of the reaction (Ha et al., 2016). The cathode stability is evaluated by ΔG_{pbx} , which measures the Gibbs free-energy distinction between the cathode and the stable regions depicted on the Pourbaix diagram (Singh et al.,

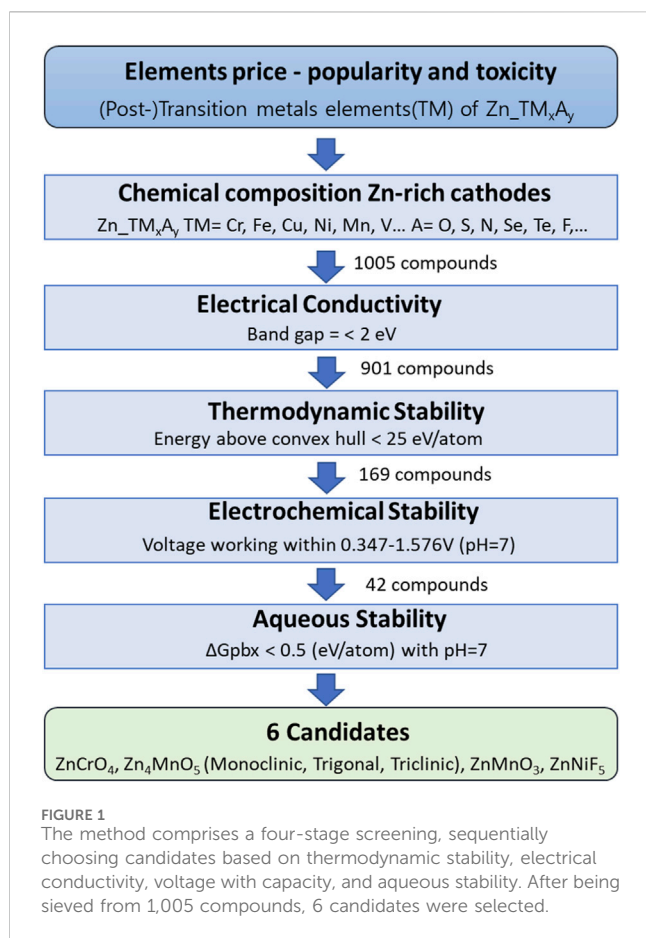
2017). This calculation is performed across a range of pH values (from 0 to 14) and potentials (from -3 to 3 V versus SHE). The investigation is conducted under typical operating conditions of AZBs, where Zn²⁺ ions are present at a concentration of 1 M and other ions at 10⁻⁶ M, ensuring relevance to real scenarios. In the expansive realm of aqueous stability, cathodes with low ΔG_{pbx} and producing solid phases as decomposition products on the Pourbaix diagram over the range of relevant potential indicate remarkable stability. These cathodes, meeting the specified criteria, often demonstrate strong operation stability. Drawing on the deep understanding provided by Singh et al., recognize that a ΔG_{pbx} less than 0.5 eV/cation (ideally approaching 0) suggests minimal reactivity in aqueous (Singh et al., 2017; Zagalskaya et al., 2023). Based on this understanding, we have chosen materials that exhibit water stability to serve as the cathodes for AFZB.

2.5 Ionic conductivity through BVPA approach

The Bond Valence Pathway Analysis (BVPA) operates as a command-line executable, and is adept at scrutinizing the energy landscape of mobile species within crystal structures (Wong et al., 2021). Leveraging Crystallographic Information Files (CIFs) and CUBE file formats generated by computational methods like Gaussian software, BVPA identifies equilibrium and interstitial sites, as well as saddle points between them. It meticulously evaluates migration paths of the lowest energy, providing detailed insights into their energetic and geometric attributes. This exhaustive inventory of migration pathways is pivotal for understanding ion transport mechanisms in solid materials (Chen et al., 2019). To bolster accessibility, BVPA is seamlessly integrated into softBV-GUI, a user-friendly graphical interface (Kabanova, 2024). This integration streamlines the invocation of both softBV and BVPA command-line programs and facilitates the interpretation of output (BVPA) through intuitive visualization tools.

2.6 High-throughput computational screening process

A systematic computational screening process has been employed to identify potential candidates for Anode-Free Zn Batteries (AFZB) from a pool of Zn-based cathode materials, as illustrated in Figure 1. To establish the molecular formula of a Zn-based cathode material, we initially proposed the formula Zn_{TM_xA_y}, where TM represents transition metals and post-transition metals, and A denotes anions. To understand the properties of each element, such as cost, abundance, and toxicity, which are critical for the practical production of cathode materials, as shown in Supplementary Table S1. Additionally, this information aims to explain the differences in the number of cathode materials formed, as observed in the initial dataset during the screening process. Initially, 1,005 compounds with the molecular formula Zn_{TM_xA_y}, where TM encompasses [Post-]transition metals including Co, Ni, Cu, Y, Zr, Sc, Ti, V, Mn, Mg, Fe, Nb, Mo, Tc, Ru, Ag, and A represents anions O, S, N, Se, Te, F, B, C, Si, P, As, Ge, were extracted from the Materials Projects database. Utilizing the Pymatgen package, 901 materials with band gaps less than 2 eV, indicative of their



ability to conduct current at room temperature, were selected for further assessment of their thermodynamic stability. The evaluation of thermodynamic stability was conducted based on Zn-based cathode materials with E_{hull} values below 25 meV/atom. Consequently, 169 compounds exhibiting phase stability were identified, meeting the criteria for use as cathode materials for AFZB. The operational voltage conditions within the H_2 evolution range (0.347 V) to the O_2 evolution range (1.578 V) at pH 7 were determined for these materials. Subsequently, 42 materials with voltage profiles falling within the standard potential range of H_2 and O_2 evolution, suitable for operation in a neutral environment, were identified. Electrochemical stability was thoroughly investigated under liquid electrolyte conditions. Utilizing the Pourbaix diagram, six compounds with an electrochemical stability energy difference (ΔG_{pbx}) less than 50 meV/atom demonstrated stability in aqueous environments, making them potential candidates. Finally, the average voltage and capacity of the most promising candidates were computed for comparison with experimental studies. This comprehensive high-throughput screening method has shown numerous advantages and conveniences in the quest for Zn-based cathode materials suitable for AFZB.

3 Results

The initial extraction process yielded 1,005 materials with the molecular formula $Zn_{TM_x}A_y$ from the Materials Project database, as illustrated in Figure 2. Transition metals, depicted in the blue

element group, are prevalent in cathode materials, constituting the majority with over 30 compounds analyzed. Among these, manganese (Mn)-based cathodes stand out as the largest group, comprising 90 compounds. Transition metals are favored as cathode materials due to their abundant presence on Earth, low production costs, enhanced safety, and ability to exist in multiple oxidation states compared to other materials. Elements in the violet-colored group include Ru, Rh, Pd, Hf, Os, Au, Pt, and Ir, known for their high cost and complex production processes. Furthermore, Cd is highly toxic element not recommended for material production. Similarly, technetium (Tc) exhibits high radioactivity, significant challenges in handling, disposal, and safety, outweighing any potential benefits they may offer in energy storage systems (Supplementary Table S1). Manganese-based cathodes have emerged as promising materials for Zn^{2+} storage in aqueous batteries, particularly in zinc batteries. Some advantages of that cathodes include affordability, low toxicity, environmental friendliness and the presence of multiple valence states (Mn^a , where $a = 0, 2+, 3+, 4+, \text{ and } 7+$). Therefore, manganese-based cathodes can effectively store and release Zn^{2+} ions during charge and discharge cycles, contributing to improved battery performance and longevity (Chen et al., 2021; Zhang et al., 2020; Zhao et al., 2020). Vanadium-based materials and their derivatives are extensively employed in zinc batteries, benefiting from abundant resources and multiple oxidation states (V^b , $b = 2+, 3+, 4+, 5+$). The diversity of polyhedral cluster structures of V_aA_b results in a variety of compositions and structures for Zn-based vanadium-based cathodes (Ding et al., 2021). In addition, Fe, Ni, and Co are commonly used metals to produce cathode materials for Zn batteries because they can enhance the performance of the oxidation and reduction reactions, leading to a higher voltage compared to MnO_2 , although they may be less stable in electrolyte environments (Gao et al., 2023). In Aqueous Zinc Batteries (ZIBs), cathodes that utilize oxide anions are particularly strongly widely often employed, primarily due to their superior capacity, structural stability, and efficient Zn^{2+} storage capabilities. Sulfur-based Zn cathodes offer high capacity but suffer from low conductivity and are susceptible to degradation in electrolyte solutions. On the other hand, Zn cathodes based on inorganic anions such as Te, As, Se, Ge, Si, and P face drawbacks including low conductivity, poor durability, and complicated fabrication (X.J. Chen et al., 2023).

In the second screening step, 901 zinc-rich cathodes were identified, all of which demonstrated a bandgap of less than 2 eV, indicating their behavior as semiconductors. This property enables these materials to facilitate electric current flow even at room temperature. Remarkably, within this subset, 75 materials exhibited metallic characteristics, characterized by a bandgap of 0 eV. These cathodes displayed high electrical conductivity, essentially functioning as conductors. Figure 3 delineates the division of the remaining 104 cathodes, separated by a red dashed line, which has a bandgap greater than 2 eV and functions as insulators. These materials necessitate higher energy or temperature conditions for electric current conduction. According to the analysis of cathode materials exhibiting a band gap of below 2 eV, as shown in Supplementary Figure S1, a larger fraction of materials still belongs to the class of elements with multivalent states rather than the other group. Furthermore,

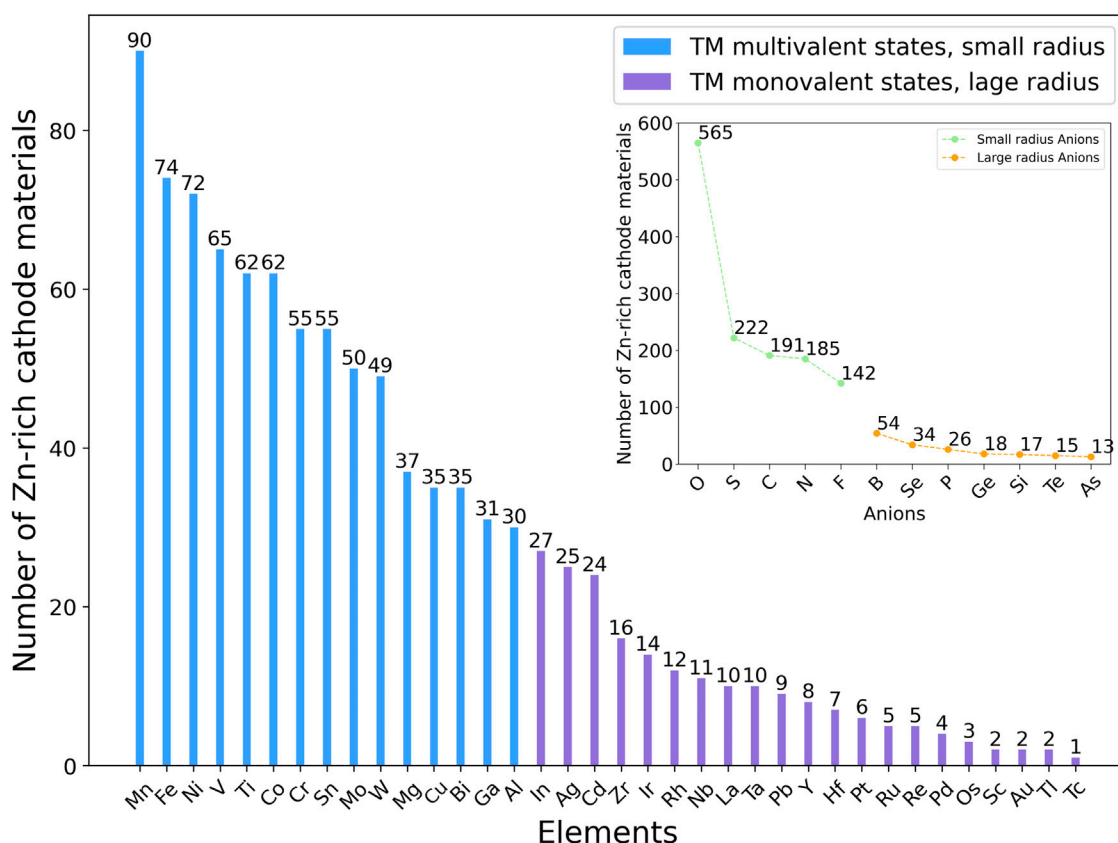


FIGURE 2

The composition of Zn-based cathode materials $\text{Zn-TM}_x\text{A}_y$ with TM includes (Post) transition metal elements; anion A such as O, S, N, Se, Te, F, B, C, Si, P, As, Ge from the Material Project database. Cathode materials containing TM in multivalent states and small radii are marked in blue. Materials containing TM in monovalent states and large radii are marked in purple. Dashed blue lines indicate cathode materials containing small radius anions, while dashed orange lines indicate cathode materials containing large radius anions.

within the band gap range of less than 0.5 eV, most cathodes primarily based on oxides exhibit a substantial reduction compared to other types of cathodes, as illustrated in [Supplementary Figure S2](#). Because oxygen has a higher electronegativity than sulfide, carbon, or nitrogen, oxygen-based cathode materials usually have a bigger band gap. This is believed to be due to oxygen attracting electrons more strongly, resulting in a larger energy difference between the lowest unoccupied molecular orbital (LUMO) and the highest occupied molecular orbital (HOMO). Anions such as sulfide, carbon, or nitrogen have lower electronegativities, resulting in higher HOMO levels and narrower band gaps in their respective materials ([Wang et al., 2021](#)). In response to the demand for optimal electrical conductivity in cathodes, a selection of 901 materials with band gap less than 2 eV was designated for an investigation into their structural robustness, electrochemical behavior, and aqueous stability.

The calculation results of energy above the hull for 901 Zn-based cathode materials are presented in [Figure 4](#). For compounds containing anion A and cation TM, the average energy above hull (E_{hull}) is calculated and colored square cells representing different energy levels are used to illustrate this process. The general trend indicates that compounds containing cations and anions with larger radii tend to have lower thermodynamic

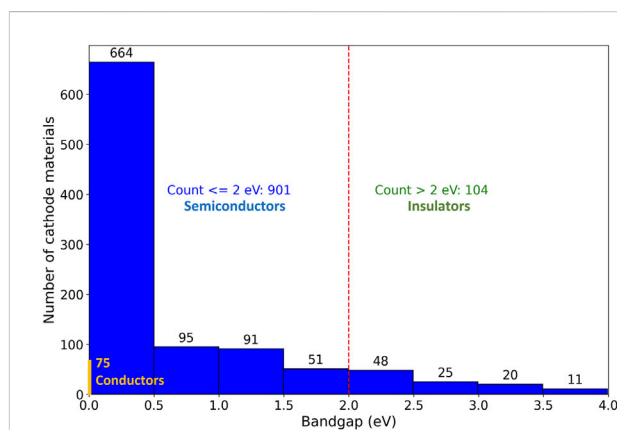


FIGURE 3

Band gaps of zinc-rich cathode materials $\text{Zn-TM}_x\text{A}_y$, where TM denotes (Post) transition metal elements and A represents anions. Dashed red lines represent a band gap value of 2 eV, dividing the cathode materials into regions of semiconductors and insulators, while solid yellow lines indicate the number of cathode materials that are conductors.

stability compared to other compounds. Notably, $\text{Zn-TM}_x\text{A}_y$ cathodes featuring small cations such as Mn (67 pm), Fe (65 pm), Ni (69 pm), Co (63 pm), Cr (69 pm), Sn (73 pm), and

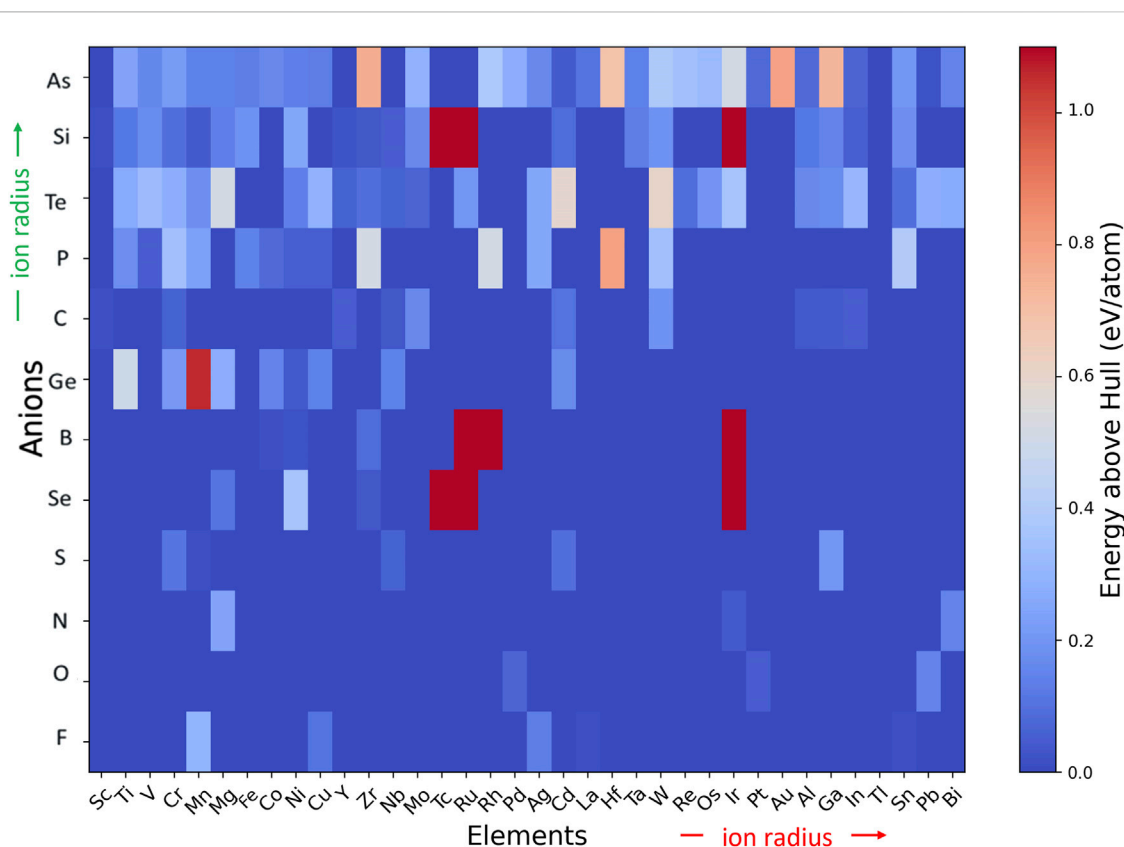


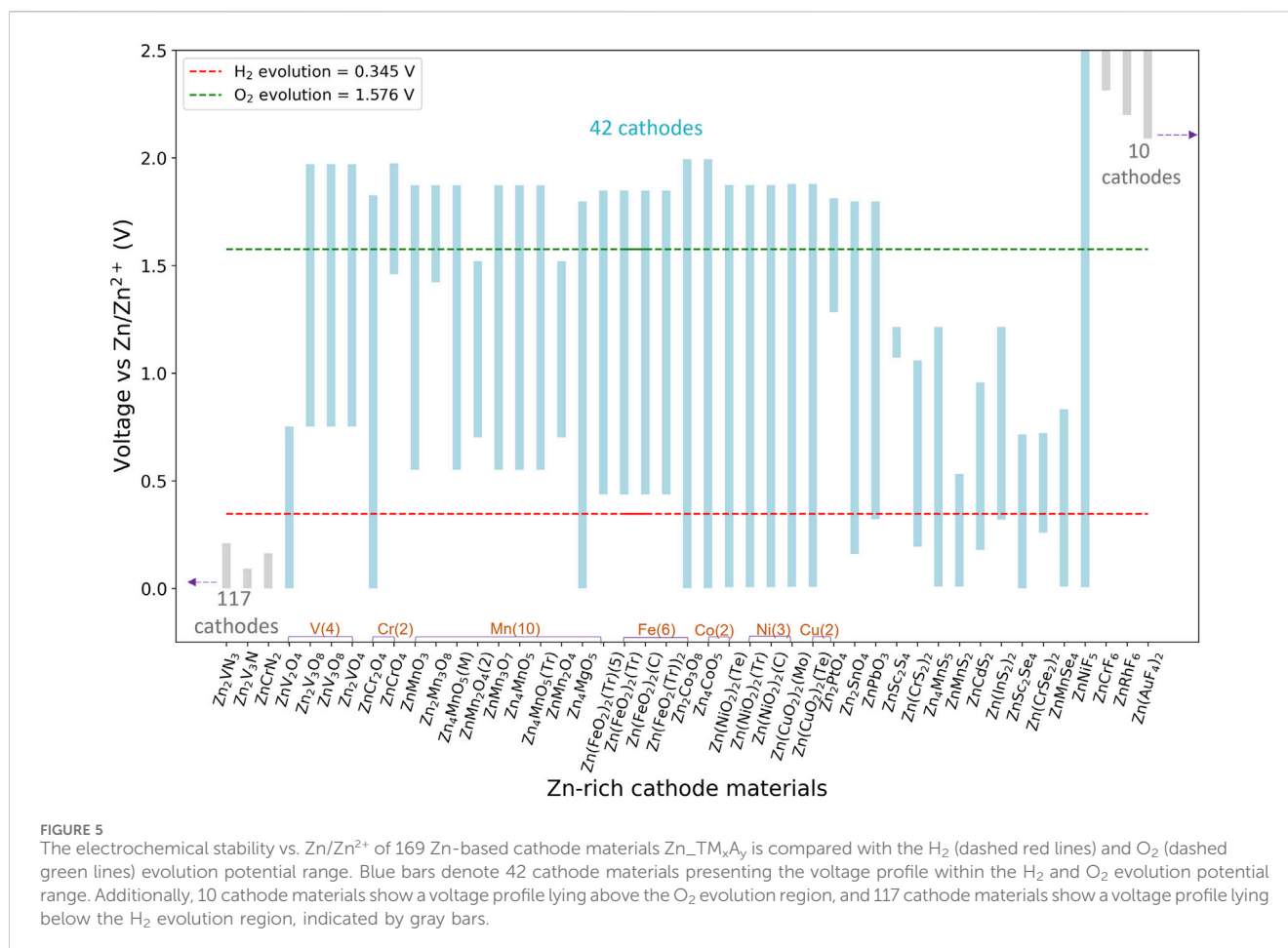
FIGURE 4

The average energy above the hull varies among 901 Zn-based cathode materials depending on the anions A and cations TM. Colored square cells represent different energy levels, while arrows indicate the increasing direction of ion radius. Most materials containing small radius anions O, S, N, C, F, and P indicate a lower average energy above the hull, exhibiting a stronger ionic bond with small cations compared to other large radius anions Se, Te, Si, P, As, and Ge.

Mg (72 pm) with relatively smaller ion radius compared to Zn (74 pm) demonstrate enhanced thermodynamic stability. Small radius cations and anions in compounds lead to enhanced bonding capability (Park et al., 2021). The number of materials for each cathode after the screening process is described in Supplementary Figure S3, all materials have energy above hull values less than 25 meV/atom, describing their thermodynamic stability. However, we also observed a clear difference between the materials based on different anions. Among them, there are 43 S-based compounds, and the number of O, N, C, and F-based materials are 41, 35, 32, and 24 respectively. On the contrary, the number of cathodes based on other anions is less, only 17 materials based on Se and P, 14 materials containing B anion, 9 materials containing Te, Ge anions, the number of materials for Si, As anion is 6 and 5, as illustrated in Supplementary Figure S4. This shows that O, N, S, and F are suitable anions to create Zn-based cathode materials with higher thermodynamic stability than other anions. The calculated energy above hull results for 169 materials with E_{hull} less than 25 meV/atom are presented in Supplementary Table S1. To explain the differences in the thermodynamic stability of Zn-based cathode materials, we analyzed how the bond strength between transition metal (TM) cations and anions (A) affects the energy above the hull. The bond strength is influenced by the charge and radius of the cations and anions. According to the rule of Pauling,

the bond strength is directly proportional to the charge and inversely proportional to the radius of the ions (Gibbs et al., 2022). Materials with smaller TM cations, such as Sc, Ti, and V, tend to form stronger ionic bonds with smaller anions like O, N, and F. This is because smaller ions can get closer together, resulting in stronger bonds. On the other hand, when these cations form bonds with larger anions, the bond strength decreases because the larger ions cannot get as close to the cations, leading to weaker bonds and higher energy above the hull. Therefore, our findings suggest that the thermodynamic stability of zinc-rich cathode materials depends on the combination of TM cations and anions, particularly the differences in their atomic radii. This understanding helps in selecting the best combinations of TM cations and anions to create new, more stable Zn-based cathode materials.

In the earlier screening, 169 Zn-based cathode materials with the general formula $\text{Zn}_x\text{TM}_y\text{A}_z$, where TM represents transition metals and A represents anions, exhibited thermodynamic stability. Following the selection based on electrochemical stability with Zn/Zn^{2+} , 42 materials were identified as potential candidates for anode-free zinc batteries (AFZB) operating in a pH 7 solution, as illustrated in Figure 5. The examination of their voltage profiles against the water decomposition process revealed that materials containing Cu, Ni, Fe, and Mn cations exhibited a broader voltage profile compared to others, suggesting their higher potential



application in AFZB. This can be explained by using the electronic flow model, in which the 3d transition metal oxides (3d TM) have suitable energy with O 2p orbitals, creating strong bonds between the TM and O atoms. From there, the TM ions can easily change valence in the discharge process. Previous studies suggest that under the assumption of uniform valence states for all TM ions, the voltage of pseudo batteries comprising TM oxides and Zn metal follows a descending sequence: $Cu > Ni > Co > Fe > Mn > Cr > V > Ti$ (Ceder et al., 1997). The tendency primarily arises from the diminishing concentration of d electrons in late TM oxides, which consequently restricts their ability to undergo valence changes. This finding enables us to select the TM anions with high operating voltage as promising cathode materials for AFZB. Furthermore, we can engineer new electrodes by combining these TM cations with other cations to enhance the voltage and the durability of the batteries. The detailed results of the electrochemical stability calculations with Zn/Zn^{2+} are presented comprehensively in Supplementary Table S2 to offer a clear insight into the screening process.

The screening of materials based on the electrochemical water stability properties of all Zn-based cathode compounds yielded 25 materials with average voltages falling within the electrochemical window of neutral water electrolysis, as depicted in Figure 6. Notably, V-based cathodes frequently display heightened reactivity with water ($\Delta G_{pbx} \geq 0.5$ eV/atom) and show

a dearth of solid decomposition products in aqueous solutions, signifying their intrinsic instability in water environments. This observation aligns with experimental findings (Wu et al., 2021). Conversely, Co, Ni, and Fe-based cathodes typically demonstrate much better stability in water, albeit with slightly lower average voltage. Cobalt, nickel, and iron ions tend to form passive oxide layers on their surfaces when exposed to air or water. These oxide layers act as protective barriers, preventing further corrosion or reactions with the surrounding environment. This passivation contributes to the stability of the cathode material in aqueous solutions (Singh et al., 2017). Observing the voltage profile of $ZnCrO_4$ compared to Zn^{2+} in Supplementary Figure S6 reveals an average voltage of 1.82 V, greater than the reduction potential of O_2 (1.576 V) in neutral pH, indicating the occurrence of the O_2 evolution process. However, $ZnCrO_4$ remains stable in aqueous environments when ΔG_{pbx} is less than 0.5 eV/atom. Therefore, in acidic electrolyte environments, $ZnCrO_4$ can be considered a potential candidate for AFZB. Moreover, manganese-based electrodes demonstrate high average voltages within the water oxidation potential window. Among the investigated materials, Zn_4MnO_5 , featuring distinct structure including monoclinic, trigonal, and triclinic, demonstrated a 1.27 V average voltage and a 270 mAh/g capacity. Conversely, as an energy density of 403.8 Wh/kg, $ZnMnO_3$ on the other hand, had the same average voltage but a greater capacity of 318 mAh/g. Manganese-based

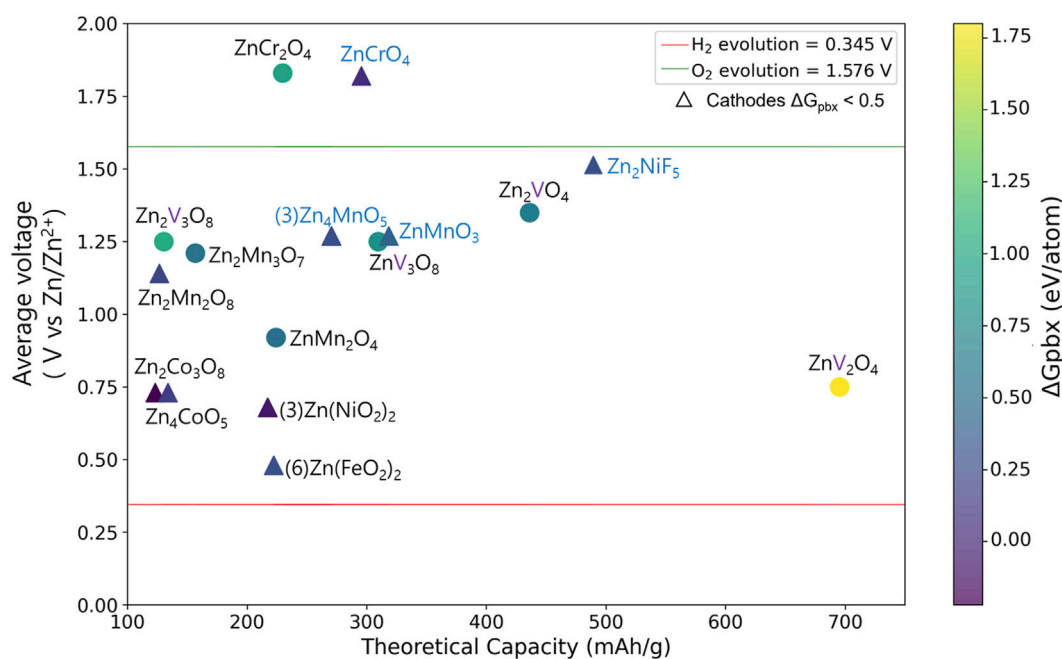


FIGURE 6

The aqueous stability of Zn-based cathode materials $Zn-TM_xA_y$ depends on ΔG_{pbx} with average voltage and theoretical capacity within the range of H_2 and O_2 evolution. Materials with ΔG_{pbx} smaller than 0.5 eV/atom are indicated by triangles, while those with ΔG_{pbx} larger than 0.5 eV/atom are indicated by circles. Candidates labeled in blue represent aqueous stability with higher average voltage and theoretical capacity than others.

cathodes, like other transition metal ions, can form passive oxide layers on their surfaces. Additionally, they exhibit good electrochemical stability, maintaining structural integrity during charge-discharge cycles in aqueous environments. This stability is further supported by their compatibility with common aqueous electrolytes used in zinc-based batteries (Zhang et al., 2020; Zhao et al., 2020). Furthermore, the promising $ZnNiF_5$ candidate has strong aqueous stability, demonstrating a remarkable 489.3 mAh/g capacity and a high average voltage of 1.52 V, suggesting its potential for cathode applications in AFZB. Observing the potential energy diagrams in Supplementary Figure S6 reveals that the average voltage of the six cathode candidates demonstrates aqueous stability with ΔG_{pbx} less than 0.5 eV/atom (indicated by triangles in Figure 6) lying within the H_2 , O_2 evolution range. Moreover, electrodes with average voltages greater than 0.5 V are considered high-voltage potential electrode materials, suitable for use as cathode materials in AFZB (Zhou et al., 2021).

Compare the energy density of the candidates from the screening process with synthetically derived materials from experiments research, as depicted in Figure 7. The pink region for Zn-based materials such as $Zn_3V_3O_8$, $ZnMn_2O_4$, $Zn_2Mo_3O_8$, $Zn_2V_2O_7$, $ZnMo_6S_8$, ZnV_2O_4 exhibited electrode capacity lower than candidates from data search such as $ZnCrO_4$, Zn_4MnO_5 (monoclinic, trigonal, triclinic), $ZnMnO_3$ and $ZnNiF_5$ (blue color region). Notably, $ZnNiF_5$ demonstrates superior energy density compared to other compounds due to its high voltage and large capacity reaching 489.31 mAh/g. The energy density of $ZnCrO_4$ is 537.79 Wh/kg, even with its relatively small capacity, owing to its high average voltage of 1.82 V. Additionally, zinc-rich cathode compounds belonging to the Mn group such as Zn_4MnO_5

(monoclinic, trigonal, triclinic) and $ZnMnO_3$, have been chosen as possible candidates due to their energy density, which is around 343 Wh/kg. With a voltage of around 1.1 V and a capacity of less than 150 mAh/g, the compound $ZnMn_3O_8$ falls short of the desired outcome and produces a rather low energy density. Compounds containing Cr and Fe elements, while water-resistant and possessing diverse structures, exhibit low average voltages, which results in a lower energy density compared to other compounds.

The utilization of a high-throughput screening method in our research has unveiled novel materials characterized by superior thermodynamic stability, voltage capacity, and aqueous durability. Supplementary Figure S5 depicts the crystal framework of these materials. These findings, as illustrated in Table 1, represent a significant stride forward. They lay a strong platform for the future development of zinc-rich electrodes, promising enhanced performance and efficiency in energy storage applications.

Figure 8 shows the ionic conductivity calculation findings for six candidates based on the $\log D - \frac{1000}{T}$ relationship with migration barrier and diffusivity statistics summarized in Supplementary Table S3. In the Arrhenius plot of Zn-ion diffusivity for Triclinic, Trigonal, and Monoclinic Zn_4MnO_5 crystal structures, diffusion coefficients of Zn^{2+} are greater than $10^{-10} \text{ cm}^2/\text{s}$, indicating fast diffusion of Zn^{2+} in these electrodes (Kabanova, 2024). Notably, the cathode electrodes of Zn_4MnO_5 with Triclinic structure exhibit faster Zn^{2+} ion conduction compared to other structures with the same formula. The same trends are observed when analyzing the results of migration energy calculations (Supplementary Table S3). On the other hand, the ion conductivity of monoclinic Zn_4MnO_5 is estimated to range from $2.2 \times 10^{-6} \text{ cm}^2/\text{s}$ to $2.6 \times 10^{-7} \text{ cm}^2/\text{s}$,

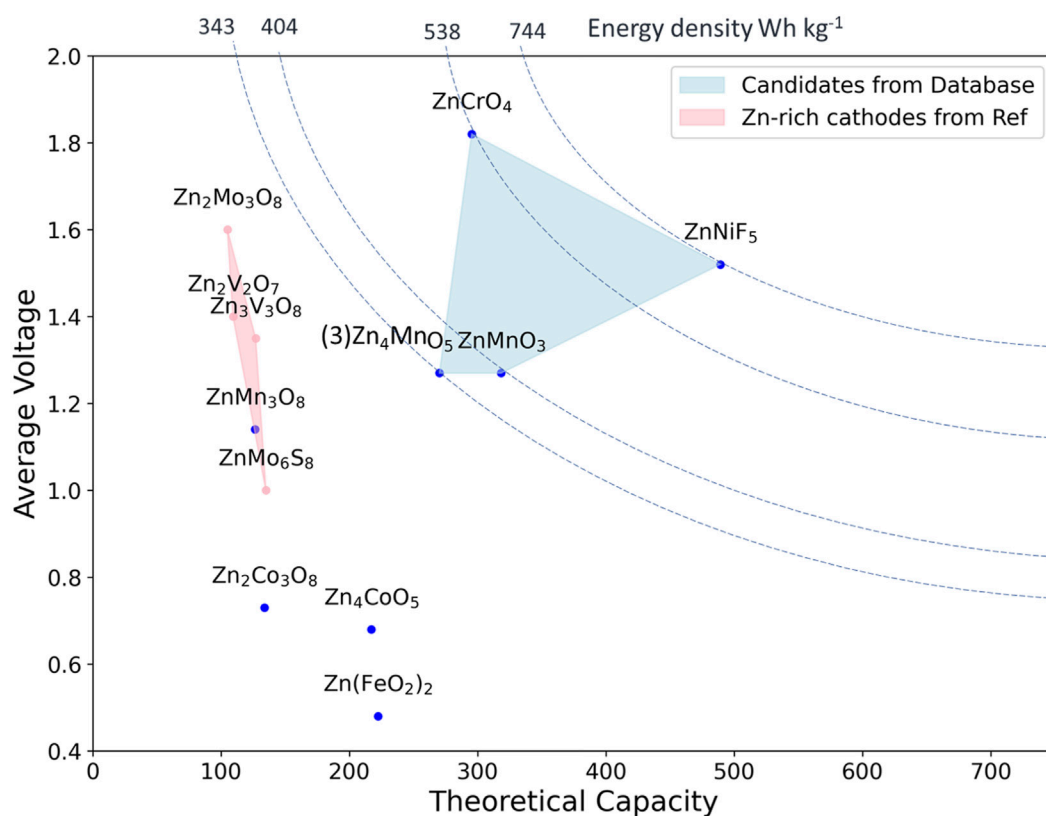


FIGURE 7

The results compare the average voltage energy with theoretical capacity of Zn-based cathode materials $Zn_{x}TM_{y}A_{z}$ from experimental research (highlighted in pink) and six candidates through high-throughput screening from the Materials Projects database (highlighted in blue). Dashed blue lines indicate the energy density calculated for the six candidates, with specific values displayed at the top of the figure.

TABLE 1 The candidates of Zn-based cathode materials for AFZB.

Composition Material-id	E_{hull}	Structure	Average voltage(V)	ΔG_{pbx} (eV/atom) (pH = 7,V)	Theo. Capacity (mAh/g)	Energy density (Wh kg ⁻¹)
ZnCrO ₄ mp-755896	0	Orthorhombic	1.82	0.05	295.49	537.79
ZnMnO ₃ mp-754318	0.006	Trigonal	1.27	0.42	318.41	403.86
Zn ₄ MnO ₅ mp-1221575	0.007	Trigonal	1.27	0.36	270.33	343.32
Zn ₄ MnO ₅ mp-1176421	0.007	Monoclinic	1.27	0.27	270.33	343.32
Zn ₄ MnO ₅ mp-773099	0.008	Triclinic	1.27	0.36	270.33	343.32
ZnNiF ₅ mp-1343278	0.021	Monoclinic	1.52	0.5	489.31	743.74

values comparable to the ion conductivity of exploited electrode materials such as Spinel Zinc cathodes material, LiCoO₂, LiMn₂O₄ (Luo et al., 2023; Park et al., 2010). Similarly, the Monoclinic structure of ZnNiF₅ shows diffusion coefficients for ion Zn²⁺ ranging from 2×10^{-11} cm²/s to 1.2×10^{-14} cm²/s, comparable to the ion conductivity of electrodes like LiFePO₄, LiFe_{1-x}Mn_xPO₄ ($0 <$

$x < 0.2$), LiZn_{0.01}Fe_{0.99}PO₄ (Park et al., 2010). Therefore, the potential of using ZnNiF₅ as a cathode electrode for AFZB can be evaluated, even though it does not exhibit rapid ion conductivity compared to Zn₄MnO₅ structures. The remaining candidate materials, ZnMnO₃ and ZnCrO₄, show difficulties in ion transport, evidenced by migration energy values of 2.054 eV and

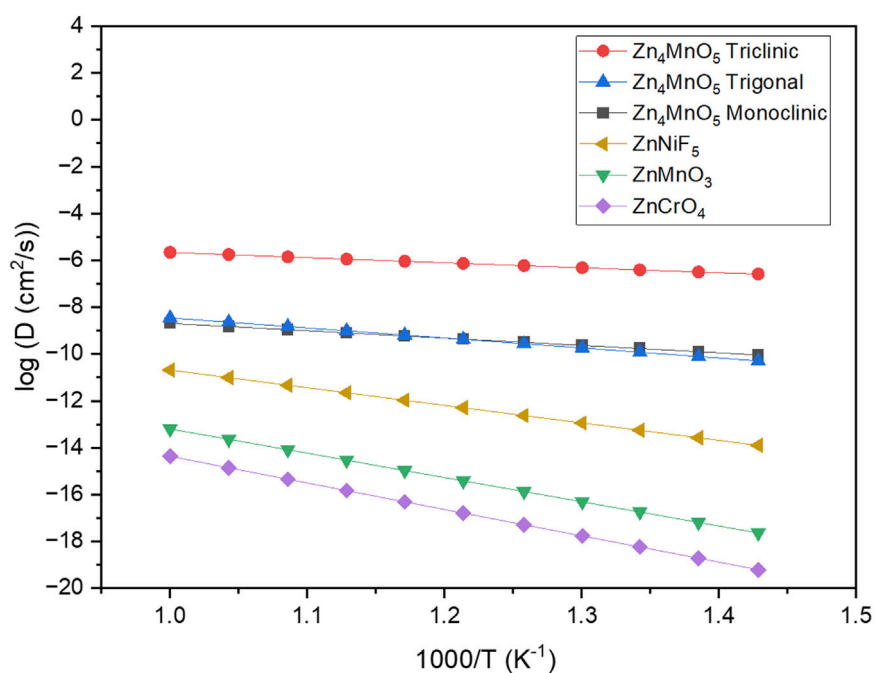


FIGURE 8 Arrhenius plots of Zn-ion diffusivity for six candidates ZnCrO_4 , Zn_4MnO_5 (Monoclinic, Trigonal, Triclinic), ZnMnO_3 , ZnNiF_5 .

2.15 eV, respectively. However, other computational methods such as Nudged Elastic Band Density Functional Theory (NEB-DFT), Ab Initio Molecular Dynamics (AIMD) simulation, generally yield much lower migration energy values compared to longer simulations at high temperatures using the BVPA (Soft BV) method (Rao et al., 2019). Hence, it can be inferred that while Zn_4MnO_5 structures display rapid ion conductivity, alternative materials like ZnMnO_3 , ZnCrO_4 , and ZnNiF_5 , despite having slightly slower ion transport kinetics, also harbor the potential to serve as suitable cathode electrodes in AFZB.

4 Discussion

Based on the high-throughput computational screening process, Zn-based cathode materials have been sequentially selected to identify potential candidates for Anode-Free Zn Batteries (AFZB). Initially, compounds with the molecular formula $\text{Zn-TM}_x\text{A}_y$ (TM includes [Post-] transition metal elements and anion A such as O, S, N, Se, Te, F, B, C, Si, P, As, Ge) were determined from the Materials Project database. Among them, $\text{Zn-TM}_x\text{A}_y$ materials containing cations Mn, Fe, Ni, V, Ti, Co, Cr, Mo, W, with low cost, multivalent states (e.g., Fe^x , $x = 0, 2+, 3+$; V^x , $x = 2+, 3+, 4+, 5+$; Mn^x , $x = 0, 2+, 3+, 4+, 7+$) constitute the majority. The cathodes are classified as semiconductors or conductors due to their electrical conductivity (band gap < 2 eV), allowing for current flow at ambient temperature. A total of 169 materials exhibited thermodynamic stability. The level of phase stability, depending on the bond strength, atomic radius of transition metal cations (TM), and anions (A). The selection of electrodes for AFZB demands high voltage within the H_2 , and O_2 evolution limits. It was observed that a variety of oxidation states for

the cations (Mn, V, Fe, Ni) expands the electrochemical stability versus Zn/Zn^{2+} compared to others. However, evaluating their aqueous stability revealed that the group of materials containing V tends to be less stable than the Mn, Fe, and Ni group. In addition to the average voltage of cathodes based on Ni and Fe being lower than Mn and Cr, the selected candidates aimed at achieving an energy density greater than 340 Wh/kg. Six materials were identified: ZnCrO_4 , monoclinic Zn_4MnO_5 , trigonal Zn_4MnO_5 , triclinic Zn_4MnO_5 , ZnMnO_3 , and ZnNiF_5 . Our method efficiently and rapidly identified and screened electrodes with outstanding electrochemical properties suitable for use as zinc-rich cathode materials.

Data availability statement

The original contributions presented in the study are included in the article/Supplementary Material, further inquiries can be directed to the corresponding author.

Author contributions

BT: Software, Investigation, Formal Analysis, Writing – review and editing, Writing – original draft, Data curation, Visualization, Conceptualization. SP: Validation, Data curation, Writing – review and editing, Visualization, Methodology, Formal Analysis. HC: Formal Analysis, Writing – review and editing, Data curation, Visualization, Methodology, Validation, Software. TM: Validation, Formal Analysis, Methodology, Data curation, Writing – review and editing, Visualization, Software. JM: Methodology, Supervision, Investigation, Software, Writing – review and editing.

Visualization, Conceptualization, Writing – original draft, Validation, Formal Analysis, Funding acquisition.

Funding

The authors declare that financial support was received for the research and/or publication of this article. This study is the result of a research project conducted with the funds of the Open R&D program of Korea Electric Power Corporation (No. R23XH03). Korea Electric Power Corporation was not involved in the study design, collection, analysis, interpretation of data, the writing of this article, or the decision to submit it for publication. This research was also supported by the National Research Foundation of Korea (NRF) grant funded by the Ministry of Science and ICT (RS-2024-00405691). This work was supported by the Technology Innovation Program (RS-2024-00449748) funded by the Ministry of Trade Industry and Energy (MOTIE, Korea). This work was supported by the Technology Innovation Program (RS-2024-00404165) through the Korea Planning and Evaluation Institute of Industrial Technology (KEIT) funded by the Ministry of Trade, Industry and Energy (MOTIE, Korea).

Conflict of interest

The authors declare that the research was conducted in the absence of any commercial or financial relationships that could be construed as a potential conflict of interest.

References

- An, Y. L., Tian, Y., Zhang, K., Liu, Y. P., Liu, C. K., Xiong, S. L., et al. (2021). Stable aqueous anode-free zinc batteries enabled by interfacial engineering. *Adv. Funct. Mater.* 31 (26), 2101886. doi:10.1002/adfm.202101886
- Aydinol, M. K., Kohan, A. F., Ceder, G., Cho, K., and Joannopoulos, J. (1997). *Ab initio* study of lithium intercalation in metal oxides and metal dichalcogenides. *Phys. Rev. B* 56 (3), 1354–1365. doi:10.1103/PhysRevB.56.1354
- Aykol, M., Dwaraknath, S. S., Sun, W., and Persson, K. A. (2018). Thermodynamic limit for synthesis of metastable inorganic materials. *Sci. Adv.* 4 (4), eaaq0148. doi:10.1126/sciadv.aqa0148
- Bartel, C. J. (2022). Review of computational approaches to predict the thermodynamic stability of inorganic solids. *J. Mater. Sci.* 57 (23), 10475–10498. doi:10.1007/s10853-022-06915-4
- Blanc, L. E., Kundu, D., and Nazar, L. F. (2020). Scientific challenges for the implementation of Zn-Ion batteries. *Joule* 4 (4), 771–799. doi:10.1016/j.joule.2020.03.002
- Boev, A. O., Fedotov, S. S., Stevenson, K. J., and Aksyonov, D. A. (2021). High-throughput computational screening of cathode materials for Li-O₂ battery. *Comput. Mater. Sci.* 197, 110592. doi:10.1016/j.commatsci.2021.110592
- Cai, J. F., Wang, Z. L., Wu, S. C., Han, Y. Q., and Li, J. J. (2021). A machine learning shortcut for screening the spinel structures of Mg/Zn ion battery cathodes with a high conductivity and rapid ion kinetics. *Energy Storage Mater.* 42, 277–285. doi:10.1016/j.ensm.2021.07.042
- Cai, K. X., Luo, S. H., Feng, J., Wang, J. C., Zhan, Y., Wang, Q., et al. (2022). Recent advances on spinel zinc manganate cathode materials for zinc-ion batteries. *Chem. Rec.* 22 (1), e202100169. doi:10.1002/tcr.202100169
- Cao, J., Zhang, D. D., Zhang, X. Y., Zeng, Z. Y., Qin, J. Q., and Huang, Y. H. (2022). Strategies of regulating Zn²⁺ solvation structures for dendrite-free and side reaction-suppressed zinc-ion batteries. *Energy and Environ. Sci.* 15 (2), 499–528. doi:10.1039/d1ee03377h
- Ceder, G., Aydinol, M. K., and Kohan, A. F. (1997). Application of first-principles calculations to the design of rechargeable Li-batteries. *Comput. Mater. Sci.* 8 (1-2): 161–169. doi:10.1016/S0927-0256(97)00029-3
- Cerqueira, T. F. T., Lin, S., Amsler, M., Goedecker, S., Botti, S., and Marques, M. A. L. (2015). Identification of Novel Cu, Ag, and Au Ternary Oxides from Global Structural Prediction. *Chem. Mater.* 27 (13), 4562–4573. doi:10.1021/acs.chemmater.5b00716
- Chen, H. M., Wong, L. L., and Adams, S. (2019). *SoftBV* – a software tool for screening the materials genome of inorganic fast ion conductors. *Acta Crystallogr. Sect. B-Structural Sci. Cryst. Eng. Mater.* 75, 18–33. doi:10.1107/S2052520618015718
- Chen, Z., Wang, P. P., Ji, Z. Y., Wang, H., Liu, J., Wang, J. Q., et al. (2020). High-voltage flexible aqueous Zn-Ion battery with extremely low dropout voltage and super-flat platform. *Nano-Micro Lett.* 12 (1), 75. doi:10.1007/s40820-020-0414-6
- Chen, D., Lu, M. J., Cai, D., Yang, H., and Han, W. (2021). Recent advances in energy storage mechanism of aqueous zinc-ion batteries. *J. Energy Chem.* 54, 712–726. doi:10.1016/j.jechem.2020.06.016
- Chen, X. J., Li, W., Reed, D., Li, X. L., and Liu, X. B. (2023). On energy storage chemistry of aqueous Zn-Ion batteries: from cathode to anode. *Electrochem. Energy Rev.* 6 (1), 33. doi:10.1007/s41918-023-00194-6
- Curtarolo, S., Setyawan, W., Hart, G. L. W., Jahnatek, M., Chepulskii, R. V., Taylor, R. H., et al. (2012). AFLOW: an automatic framework for high-throughput materials discovery. *Comput. Mater. Sci.* 58, 218–226. doi:10.1016/j.commatsci.2012.02.005
- Curtarolo, S., Hart, G. L. W., Nardelli, M. B., Mingo, N., Sanvito, S., and Levy, O. (2013). The high-throughput highway to computational materials design. *Nat. Mater.* 12 (3), 191–201. doi:10.1038/Nmat3568
- Ding, J. W., Gao, H. G., Ji, D. F., Zhao, K., Wang, S. W., and Cheng, F. Y. (2021). Vanadium-based cathodes for aqueous zinc-ion batteries: from crystal structures, diffusion channels to storage mechanisms. *J. Mater. Chem. A* 9 (9), 5258–5275. doi:10.1039/d0ta10336e
- Du, W. C., Huang, S., Zhang, Y. F., Ye, M. H., and Li, C. C. (2022). Enable commercial zinc powders for dendrite-free zinc anode with improved utilization rate by pristine graphene hybridization. *Energy Storage Mater.* 45, 465–473. doi:10.1016/j.ensm.2021.12.007
- Fang, G. Z., Zhou, J., Pan, A. Q., and Liang, S. Q. (2018). Recent advances in aqueous zinc-ion batteries. *ACS Energy Lett.* 3 (10), 2480–2501. doi:10.1021/acsenenergyl.8b01426

Generative AI statement

The authors declare that Generative AI was used in the creation of this manuscript. Portions of the language editing and formatting of this manuscript were assisted by OpenAI's ChatGPT, under the supervision and verification of the authors. The scientific content and data analysis were entirely conducted by the authors.

Any alternative text (alt text) provided alongside figures in this article has been generated by Frontiers with the support of artificial intelligence and reasonable efforts have been made to ensure accuracy, including review by the authors wherever possible. If you identify any issues, please contact us.

Publisher's note

All claims expressed in this article are solely those of the authors and do not necessarily represent those of their affiliated organizations, or those of the publisher, the editors and the reviewers. Any product that may be evaluated in this article, or claim that may be made by its manufacturer, is not guaranteed or endorsed by the publisher.

Supplementary material

The Supplementary Material for this article can be found online at: <https://www.frontiersin.org/articles/10.3389/fbael.2025.1723256/full#supplementary-material>

- Gao, F. F., Shi, W. C., Jiang, B. W., Xia, Z. Z., Zhang, L., and An, Q. Y. (2023). Ni/Fe bimetallic ions Co-Doped manganese dioxide cathode materials for aqueous zinc-ion batteries. *Batteries* 9 (1), 50. doi:10.3390/batteries9010050
- Gibbs, G. V., Hawthorne, F. C., and Brown, G. E. (2022). Pauling's rules for oxide-based minerals: a re-examination based on quantum mechanical constraints and modern applications of bond-valence theory to Earth materials. *Am. Mineralogist* 107 (7), 1219–1248. doi:10.2138/am-2021-7938
- Gong, M., Li, Y. G., Zhang, H. B., Zhang, B., Zhou, W., Feng, J., et al. (2014). Ultrafast high-capacity NiZn battery with NiAlCo-layered double hydroxide. *Energy and Environ. Sci.* 7 (6), 2025–2032. doi:10.1039/c4ee00317a
- Guo, P. S., Yang, G. Z., and Wang, C. X. (2021). Electrochemically-induced structural reconstruction in promoting the Zn storage performance of a CaMn₂O₆ cathode for superior long-life aqueous Zn-ion batteries. *J. Mater. Chem. A* 9 (31), 16868–16877. doi:10.1039/d1ta03708k
- Ha, J. M., Wang, Z. B., Novitskaya, E., Hirata, G. A., Graeve, O. A., Ong, S. P., et al. (2016). An integrated first principles and experimental investigation of the relationship between structural rigidity and quantum efficiency in phosphors for solid state lighting. *J. Luminescence* 179, 297–305. doi:10.1016/j.jlumin.2016.07.006
- Hart, G. L. W., and Forcade, R. W. (2008). Algorithm for generating derivative structures. *Phys. Rev. B* 77 (22), 224115. doi:10.1103/PhysRevB.77.224115
- Hautier, G., Ong, S. P., Jain, A., Moore, C. J., and Ceder, G. (2012). Accuracy of density functional theory in predicting formation energies of ternary oxides from binary oxides and its implication on phase stability. *Phys. Rev. B* 85, 155208. doi:10.1103/PhysRevB.85.155208
- Jain, A., Ong, S. P., Hautier, G., Chen, W., Richards, W. D., Dacek, S., et al. (2013). Commentary: the materials project: a materials genome approach to accelerating materials innovation. *Apl. Mater.* 1 (1), 011002. doi:10.1063/1.4812323
- Jia, X. X., Liu, C. F., Neale, Z. G., Yang, J. H., and Cao, G. Z. (2020). Active materials for aqueous zinc ion batteries: synthesis, crystal structure, morphology, and electrochemistry. *Chem. Rev.* 120 (15), 7795–7866. doi:10.1021/acs.chemrev.9b00628
- Kabanova, N. A. (2024). Theoretical study of the oxygen ion conductivity and modeling new hollandite-type structures LnM₆O₁₂ (Ln = Pr, Nd; M = Ti, Nb, Mo). *Comput. Theor. Chem.* 1234, 114516. doi:10.1016/j.comptc.2024.114516
- Kabiraj, A., and Mahapatra, S. (2022). High-Throughput Assessment of Two-Dimensional Electrode Materials for Energy Storage Devices. *Cell Rep. Phys. Sci.* 3 (1), 100718. doi:10.1016/j.xcrp.2021.100718
- Kahle, L., Marcolongo, A., and Marzari, N. (2020). High-throughput computational screening for solid-state Li-ion conductors. *Energy and Environ. Sci.* 13 (3), 928–948. doi:10.1039/c9ee02457c
- Kasiri, G., Glenneberg, J., Bani Hashemi, A., Kun, R., and La Mantia, F. (2019). Mixed copper-zinc hexacyanoferrates as cathode materials for aqueous zinc-ion batteries. *Energy Storage Mater.* 19, 360–369. doi:10.1016/j.ensm.2019.03.006
- Knight, J. C., Therese, S., and Manthiram, A. (2015). Chemical extraction of Zn from ZnMn₂O₄-based spinels. *J. Mater. Chem. A* 3 (42), 21077–21082. doi:10.1039/c5ta06482a
- Kundu, D., Adams, B. D., Duffort, V., Vajargah, S. H., and Nazar, L. F. (2016). A high-capacity and long-life aqueous rechargeable zinc battery using a metal oxide intercalation cathode. *Nat. Energy* 1, 16119. doi:10.1038/Nenergy.2016.119
- Li, M., Lu, J., Ji, X. L., Li, Y. G., Shao, Y. Y., Chen, Z. W., et al. (2020). Design strategies for nonaqueous multivalent-ion and monovalent-ion battery anodes. *Nat. Rev. Mater.* 5 (4), 276–294. doi:10.1038/s41578-019-0166-4
- Li, B., Zhang, X. T., Wang, T. L., He, Z. X., Lu, B. A., Liang, S. Q., et al. (2022). Interfacial Engineering Strategy for High-Performance Zn Metal Anodes. *Nano-Micro Lett.* 14 (1), 6. doi:10.1007/s40820-021-00764-7
- Lin, L. D., Qin, K., Hu, Y. S., Li, H., Huang, X. J., Suo, L. M., et al. (2022). A Better Choice to Achieve High Volumetric Energy Density: Anode-Free Lithium-Metal Batteries. *Adv. Mater.* 34 (23), 2110323. doi:10.1002/adma.202110323
- Liu, Y., and Wu, X. (2022). Strategies for constructing manganese-based oxide electrode materials for aqueous rechargeable zinc-ion batteries. *Chin. Chem. Lett.* 33 (3), 1236–1244. doi:10.1016/j.ccllet.2021.08.081
- Luo, H. R., Deng, J. B., Gou, Q. Z., Odunmbaku, O., Sun, K., Xiao, J. X., et al. (2023). Accelerated discovery of novel high-performance zinc-ion battery cathode materials by combining high-throughput screening and experiments. *Chin. Chem. Lett.* 34 (8), 107885. doi:10.1016/j.ccllet.2022.107885
- Ming, F. W., Zhu, Y. P., Huang, G., Emwas, A. H., Liang, H. F., Cui, Y., et al. (2022). Co-Solvent Electrolyte Engineering for Stable Anode-Free Zinc Metal Batteries. *J. Am. Chem. Soc.* 144 (16), 7160–7170. doi:10.1021/jacs.1c12764
- Ong, S. P., Wang, L., Kang, B., and Ceder, G. (2008). Li-Fe-P-O₂ Phase Diagram from First Principles Calculations. *Chem. Mater.* 20 (5), 1798–1807. doi:10.1021/cm702327g
- Ong, S. P., Richards, W. D., Jain, A., Hautier, G., Kocher, M., Cholia, S., et al. (2013). Python Materials Genomics (pymatgen): A robust, open-source python library for materials analysis. *Comput. Mater. Sci.* 68, 314–319. doi:10.1016/j.commatsci.2012.10.028
- Pan, C. S., Nuzzo, R. G., and Gewirth, A. A. (2017). ZnAl_xCo_{2-x}O₄ Spinel as Cathode Materials for Non-Aqueous Zn Batteries with an Open Circuit Voltage of ≤2 V. *Chem. Mater.* 29 (21), 9351–9359. doi:10.1021/acs.chemmater.7b03340
- Park, M., Zhang, X. C., Chung, M. D., Less, G. B., and Sastry, A. M. (2010). A review of conduction phenomena in Li-ion batteries. *J. Power Sources* 195 (24), 7904–7929. doi:10.1016/j.jpowsour.2010.06.060
- Park, D., Kim, K., Chun, G. H., Wood, B. C., Shim, J. H., and Yu, S. (2021). Materials design of sodium chloride solid electrolytes Na₃MCl₆ for all-solid-state sodium-ion batteries. *J. Mater. Chem. A* 9 (40), 23037–23045. doi:10.1039/d1ta07050a
- Persson, K. A., Waldwick, B., Lazic, P., and Ceder, G. (2012). Prediction of solid-aqueous equilibria: Scheme to combine first-principles calculations of solids with experimental aqueous states. *Phys. Rev. B* 85 (23), 235438. doi:10.1103/PhysRevB.85.235438
- Prasad Rao, R., Chen, H. M., and Adams, S. (2019). Stable Lithium Ion Conducting Thiophosphate Solid Electrolytes Li_x(PS₄)_x (X = Cl, Br, I). *Chem. Mater.* 31 (21), 8649–8662. doi:10.1021/acs.chemmater.9b01926
- Qian, J. F., Adams, B. D., Zheng, J. M., Xu, W., Henderson, W. A., Wang, J., et al. (2016). Anode-Free Rechargeable Lithium Metal Batteries. *Adv. Funct. Mater.* 26 (39), 7094–7102. doi:10.1002/adfm.201602353
- Ricci, F., Dunn, A., Jain, A., Rignanese, G. M., and Hautier, G. (2020). Gapped metals as thermoelectric materials revealed by high-throughput screening. *J. Mater. Chem. A* 8 (34), 17579–17594. doi:10.1039/d0ta05197g
- Shen, L., Wang, Z., Xu, S., Law, H. M., Zhou, Y., and Ciucci, F. (2025). Harnessing Database-Supported High-Throughput Screening for the Design of Stable Interlayers in Halide-Based All-Solid-State Batteries. *Nat. Commun.* 16, 3687. doi:10.1038/s41467-025-58522-x
- Singh, A. K., Zhou, L., Shinde, A., Suram, S. K., Montoya, J. H., Winston, D., et al. (2017). Electrochemical Stability of Metastable Materials. *Chem. Mater.* 29 (23), 10159–10167. doi:10.1021/acs.chemmater.7b03980
- Song, M., Tan, H., Chao, D. L., and Fan, H. J. (2018). Recent Advances in Zn-Ion Batteries. *Adv. Funct. Mater.* 28 (41), 1802564. doi:10.1002/adfm.201802564
- Sun, W., Dacek, S. T., Ong, S. P., Hautier, G., Jain, A., Richards, W. D., et al. (2016). The Thermodynamic Scale of Inorganic Crystalline Metastability. *Sci. Adv.* 2 (11), e1600225. doi:10.1126/sciadv.1600225
- Wang, S. B., Ding, Z. X., and Wang, X. C. (2015). A stable ZnCo₂O₄cocatalyst for photocatalytic CO₂reduction. *Chem. Commun.* 51 (8), 1517–1519. doi:10.1039/c4cc07225a
- Wang, F., Borodin, O., Gao, T., Fan, X. L., Sun, W., Han, F. D., et al. (2018). Highly reversible zinc metal anode for aqueous batteries. *Nat. Mater.* 17 (6), 543–549. doi:10.1038/s41563-018-0063-z
- Wang, C., Song, Z. H., Shi, P., Lv, L., Wan, H. Z., Tao, L., et al. (2021). High-rate transition metal-based cathode materials for battery-supercapacitor hybrid devices. *Nanoscale Adv.* 3 (18), 5222–5239. doi:10.1039/d1na00523e
- Wang, Z. Y., Zhu, H., Ai, L., Ding, J. M., Zhu, P. F., Li, Z. Q., et al. (2021). Synthesis, Electronic Structure, and Electrochemical Properties of the Cubic Mg₂MnO₄ Spinel with Porous-Spongy Structure. *Nanomaterials* 11 (5), 1122. doi:10.3390/nano11051122
- Wang, G., Zhu, M. S., Chen, G. B., Qu, Z., Kohn, B., Scheler, U., et al. (2022). An Anode-Free Zn-Graphite Battery. *Adv. Mater.* 34 (29), 2201957. doi:10.1002/adma.202201957
- Wong, L. L., Phuah, K. C., Dai, R. Y., Chen, H. M., Chew, W. S., and Adams, S. (2021). Bond Valence Pathway Analyzer-An Automatic Rapid Screening Tool for Fast Ion Conductors within softBV. *Chem. Mater.* 33 (2), 625–641. doi:10.1021/acs.chemmater.0c03893
- Wu, J., Kuang, Q., Zhang, K., Feng, J. J., Huang, C. M., Li, J. J., et al. (2021). Spinel Zn₃V₃O₈: A high-capacity zinc supplied cathode for aqueous Zn-ion batteries. *Energy Storage Mater.* 41, 297–309. doi:10.1016/j.ensm.2021.06.006
- Xie, Y., Jin, Y. C., and Xiang, L. (2017). Understanding Mn-Based Intercalation Cathodes from Thermodynamics and Kinetics. *Crystals* 7 (7), 221. doi:10.3390/cryst7070221
- Xie, X. S., Liang, S. Q., Gao, J. W., Guo, S., Guo, J. B., Wang, C., et al. (2020). Manipulating the ion-transfer kinetics and interface stability for high-performance zinc metal anodes. *Energy and Environ. Sci.* 13 (2), 503–510. doi:10.1039/c9ee03545a
- Yang, W., Yang, W., Huang, Y. F., Xu, C. J., Dong, L. B., and Peng, X. W. (2022). Reversible aqueous zinc-ion battery based on ferric vanadate cathode. *Chin. Chem. Lett.* 33 (10), 4628–4634. doi:10.1016/j.ccllet.2021.12.049
- Young, S. D., Chen, J. D., Sun, W. H., Goldsmith, B. R., and Pilania, G. (2023). Thermodynamic Stability and Anion Ordering of Perovskite Oxynitrides. *Chem. Mater.* 35 (15), 5975–5987. doi:10.1021/acs.chemmater.3c00943
- Zagalskaya, A., Chaudhary, P., and Alexandrov, V. (2023). Corrosion of Electrochemical Energy Materials: Stability Analyses beyond Pourbaix Diagrams. *J. Phys. Chem. C* 127 (30), 14587–14598. doi:10.1021/acs.jpcc.3c01727
- Zanatta, A. R. (2019). Revisiting the optical bandgap of semiconductors and the proposal of a unified methodology to its determination. *Sci. Rep.* 9, 11225. doi:10.1038/s41598-019-47670-y

- Zhang, N., Cheng, F. Y., Liu, Y. C., Zhao, Q., Lei, K. X., Chen, C. C., et al. (2016). Cation-Deficient Spinel $ZnMn_2O_4$ Cathode in $Zn(CF_3SO_3)_2$ Electrolyte for Rechargeable Aqueous Zn-Ion Battery. *J. Am. Chem. Soc.* 138 (39), 12894–12901. doi:10.1021/jacs.6b05958
- Zhang, H. Z., Wang, J., Liu, Q. Y., He, W. Y., Lai, Z. Z., Zhang, X. Y., et al. (2019). Extracting oxygen anions from $ZnMn_2O_4$: Robust cathode for flexible all-solid-state Zn-ion batteries. *Energy Storage Mater.* 21, 154–161. doi:10.1016/j.ensm.2018.12.019
- Zhang, Q. C., Li, C. W., Li, Q. L., Pan, Z. H., Sun, J., Zhou, Z. Y., et al. (2019). Flexible and High-Voltage Coaxial-Fiber Aqueous Rechargeable Zinc-Ion Battery. *Nano Lett.* 19 (6), 4035–4042. doi:10.1021/acs.nanolett.9b01403
- Zhang, N., Chen, X. Y., Yu, M., Niu, Z. Q., Cheng, F. Y., and Chen, J. (2020). Materials chemistry for rechargeable zinc-ion batteries. *Chem. Soc. Rev.* 49 (13), 4203–4219. doi:10.1039/c9cs00349e
- Zhang, C., Shin, W., Zhu, L. D., Chen, C., Neufeind, J. C., Xu, Y. K., et al. (2021). The electrolyte comprising more robust water and superhalides transforms Zn-metal anode reversibly and dendrite-free. *Carbon Energy* 3 (2), 339–348. doi:10.1002/cey2.70
- Zhang, Y. X., Wang, L. Q., Li, Q. Y., Hu, B., Kang, J. M., Meng, Y. H., et al. (2022). Iodine Promoted Ultralow Zn Nucleation Overpotential and Zn-Rich Cathode for Low-Cost, Fast-Production and High-Energy Density Anode-Free Zn-Iodine Batteries. *Nano-Micro Lett.* 14 (1), 208. doi:10.1007/s40820-022-00948-9
- Zhao, Z. M., Zhao, J. W., Hu, Z. L., Li, J. D., Li, J. J., Zhang, Y. J., et al. (2019). Long-life and deeply rechargeable aqueous Zn anodes enabled by a multifunctional brightener-inspired interphase. *Energy and Environ. Sci.* 12 (6), 1938–1949. doi:10.1039/c9ee00596j
- Zhao, Q. H., Song, A. Y., Ding, S. X., Qin, R. Z., Cui, Y. H., Li, S. N., et al. (2020). Preintercalation Strategy in Manganese Oxides for Electrochemical Energy Storage: Review and Prospects. *Adv. Mater.* 32 (50), 2002450. doi:10.1002/adma.202002450
- Zhao, Y. L., Zhu, Y. H., and Zhang, X. B. (2020). Challenges and perspectives for manganese-based oxides for advanced aqueous zinc-ion batteries. *Infomat* 2 (2), 237–260. doi:10.1002/inf2.12042
- Zheng, J. X., Zhao, Q., Tang, T., Yin, J. F., Quilty, C. D., Renderos, G. D., et al. (2019). Reversible epitaxial electrodeposition of metals in battery anodes. *Science* 366 (6465), 645–648. doi:10.1126/science.aax6873
- Zhou, L. M., Yao, A. M. Z., Wu, Y. J., Hu, Z. Y., Huang, Y. H., and Hong, Z. J. (2021). Machine Learning Assisted Prediction of Cathode Materials for Zn-Ion Batteries. *Adv. Theory Simulations* 4 (9), 2100196. doi:10.1002/adts.202100196
- Zhu, Y. P., Cui, Y., and Alshareef, H. N. (2021). An Anode-Free Zn-MnO₂ Battery. *Nano Lett.* 21 (3), 1446–1453. doi:10.1021/acs.nanolett.0c04519